The Undrained Behavior of Drilled Shaft Foundations Subjected to Static Inclined Loading

정적 경사하중을 받는 현장타설말뚝기초의 비배수 거동

Cho, Nam-Jun*1
조 남 준
Kulhawy, Fred H.*2

요 지

현장타설말뚝기초가 보다 빈번하게 여러가지 구조물의 기초로 쓰이고 있다. 그러나, 경사하중하의 현장타설말뚝의 거동에 대하여는 알려진 사실이 거의 없다. 본 연구에서는, 경사하중을 받는 현장타설말뚝의 비배수거동에 대하여 연구하고자 체계적인 실험을 행하였다. 기초의 직경에 대한 깊이의 비와 하중의 경사도가 같은 변수들을 변화시키면서 행한 연구를 통하여 경사하중에 대한 지지력을 예측하는 반이론적 방법을 개발하였다. 시험변수들은 실제 송전탑건설시 가장 빈번하게 사용되는 대표적인 값들과 같도록 선택되었다. 직경에 대한 말뚝의 깊이비(D/B)가 서로 다른 짧은 강체말뚝에 대하여 논하였으며, 축방향 인발, 경사 인발, 그리고 경사 압축등과 같은 하중상태에 대하여 연구하였다. 경사지지력을 구조상호작용 방정식과 본 실험연구에서 개발한 공식을 사용하여 평가하여 보았다. 본 연구에서 개발한 새로운 공식은 실험실 시험치와, 제한적이나마, 현장의 실제시험치에 적용될 수 있음을 알 수 있었다.

Abstract

Drilled shafts are used increasingly as the foundations for many types of structures. However, very little knowledge of drilled shaft behavior under inclined load is available. In this study, a systematic experimental testing program was conducted to understand the undrained behavior of drilled shaft foundations under inclined loads. A semi-theoretical method of predicting the inclined capacity was developed through a parametric study of the variables such as shaft geometry and load inclination. Test parameters were chosen to be representative of those most frequently used in the electric utility industry. Short, rigid shafts with varying depth/diameter(D/B) ratios were addressed, and loading modes were investigated that included axial uplift, inclined uplift, and inclined compression loads. Capacities were evaluated using the structural interaction formula and an equation developed from this experimental study. This new equation models the laboratory data well and is applicable for the limited field data.

*1 정회원, 국민대학교 공과대학 토목환경공학과 전임강사

*2 Professor, School of Civil and Environ mental Engineering,

1. Introduction

Depending on the geometry and type of structures, different combinations of loads would be transmitted to the foundations. The foundations for truss towers like transmission line structures are often subjected to inclined loading. The inclined load in this study is defined as the applied load with a constant inclination during loading.

Because of nonlinear soil behavior and the nonsymmetric three−dimensional nature of the problem, a very complex theoretical approach would result for analyzing the behavior of drilled shaft foundations under inclined loads. Therefore, only approximate theoretical and semiempirical solutions have been suggested by several authors. Most of these solutions were developed for predicting the inclined capacity of driven piles, and therefore they may be of limited applicability to drilled shafts. Furthermore, most of the available studies have been conducted on the behavior of driven or bored piles under inclined loads in sand [1, 3, 8, 24, 25, 26]. However, they provide useful background for the analysis of inclined load tests in clay.

2. Theoretical Background

Figures 1a and 1b show simplified diagrams representing models of free−headed deep foundations in clay, subjected to inclined compression and uplift load, respectively, and the corresponding soil stress conditions[20]. For these models, the net lateral soil stresses on the embedded shaft, H_1 and H_2, were assumed to have approximately rectangular and triangular stress distributions, respectively. The lateral bearing factors($N_{\Psi p}$) for inclined loading can vary from zero at a load inclination(Ψ) of 0 (axial uplift) or 180 degrees (axial compression), which are measured from the upward vertical axis, to the lateral bearing factor for pure lateral loading (N_p at Ψequal to 90 degrees. Therefore, the H_1 and H_2 forces increase as Ψ deviates more from the vertical axis.

For undrained analysis($\phi=0$), it may be necessary to introduce the concept of an apparent side contact area(A_Ψ) to evaluate the side resistance of a shaft subjected to inclined loads. For $\Psi=0$ or 180 degrees, $A_{0° \text{ or } 180°}$ is obviously equal to πBD. For $\Psi=90$ degrees, $A_{90°}$ can be assumed to be $0.5\pi BD$[5]. Therefore, the apparent side contact area (A_Ψ) for arbitrary load inclinations can be assumed to vary from $0.5\pi BD$ at $\Psi=90$ degrees to πBD at $\Psi=0$ or 180 degrees. Then, the maximum possible side resistance for an arbitray Ψ will be $s_u A_\Psi$. However, it should be noted that the undrained strength(s_u) also varies with the di rection of applied load[10]. It further should be noted that the side resistance can not reach the full side resistance ($s_u A_\Psi$) if the shaft under inclined loading fails because of lack of lateral resistance, i, e., in lateral dominant loading. Therefore, it is important to note whether the dominant failure mechanism is axial or lateral.

The tip resistance($Q_{tc\omega}$) under inclined compression develops at the shaft tip at an inclination angle (ω) from the vertical. For the limits of $\Psi=180$ and 90 degrees, $\omega=0$ and 90

degrees, respectively. The tip load inclination (ω) can be expressed as follows [19]:

$$\omega = (180^\circ - \Psi)^2 / 90^\circ \tag{1}$$

in which ω and Ψ are in degrees.

The undrained tip resistance of a deep foundation under axial compression loads can be evaluated by using the bearing capacity factors defined uniquely as $N_c=5.14$, $N_\gamma=0$, and $N_q=1$. The ultimate tip resistance (q_{ult}) for axial compression is presented elsewhere[11]. The tip resistance under inclined compression load ($Q_{t\psi\omega}$) can vary from $\alpha_t s_u A_t$ at $\Psi=90$ degrees to $q_{ult}A_t$ at $\Psi=180$ dgrees, respecively, in which α_t=adhesion factor at tip and A_t=tip area. Therefore, the vertical component of tip resistance ($Q_{t\psi\omega}\cos^m$) will vary from zero at $\Psi=90$ degrees (or $\omega=90$ degrees) to $q_{ult}A_t$ at $\Psi=180$ degrees (or $\omega=0$ degrees), respectively. Also, it must be noted that s_u, which is used for calculating s_uA_t an q_{ult}, is highly dependent on the loading mode and boundary conditions[10].

The inclined loading effect on bearing capacity can be addressed using inclination factors proposed by several authors[6, 16, 23]. For inclined compression, the bearing capacity factors N_γ, N_c, and N_q should be modified by multiplying by the corresponding inclination factors. This approach is simple and straightforward because only the conventional bearing capacity and load inclination factors are needed to calculate the inclined capacity. However, it should be noted that the lateral resistance of the foundation should be considered in evaluating the inclined capacity because the inclined capacity is a combination of both vertical and lateral reactions.

Although previous studies[20] established the force diagram in Figure 1 semitheoretically, they did not calculate the inclined capacity directly from the diagram because of the difficulty and complexity involved in calculating each force. Therefore, the prediction of inclined compression capacity can be accomplished using a well-known structural interaction formula, given as follows[18]:

$$(P_{\psi c}\cos\Psi / Q_c)^2 + (P_{\psi c}\sin\Psi / H_u)^2 = 1 \tag{2}$$

in which $P_{\psi c}$=inclined compression capacity, Ψ=applied load inclination, Q_c=axial compression capacity, and H_u=lateral capacity. Detailed methods for evaluating the axial compression capacity and the lateral capacity of drilled shafts are given elsewhere[11, 14].

It has been suggested that the analysis for anchor walls under inclined uplift load can be used to calculate the inclined uplift capacity ($P_{\psi u}$) of rigid piles by utilizing the shape factors for the piles[17]. Then $P_{\psi u}$ can be evauated as follows:

$$P_{\psi u} = (\alpha c K_{cu} D + \gamma D^2 K_{bu}/2)B + W\cos\Psi \tag{3}$$

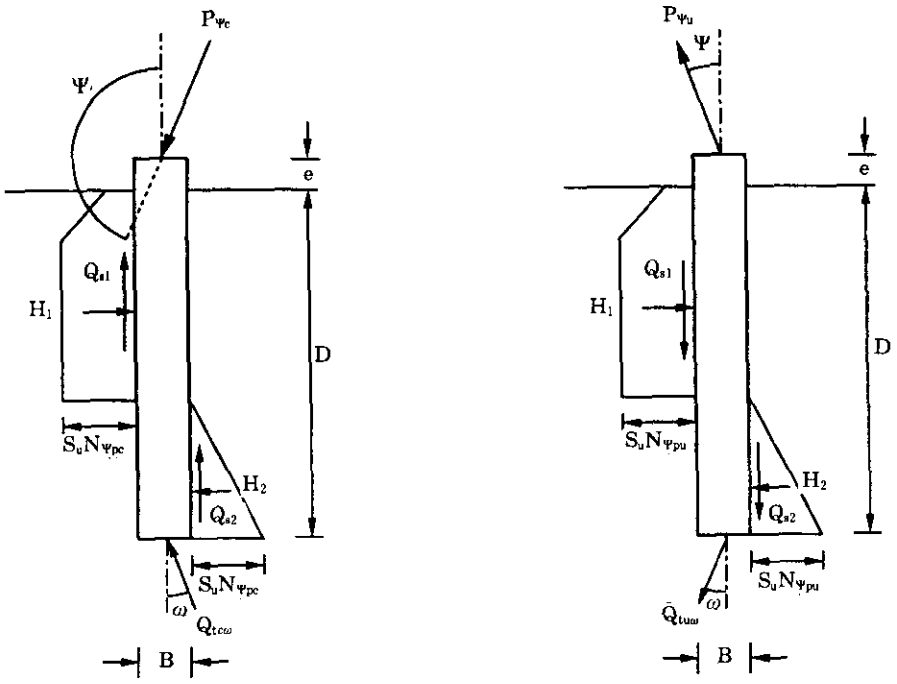

(a) Compression load and

(b) Uplift load

Figure.1 Simplified force diagram of single rigid shaft under inclined

in which α=adhesion factor, c=cohesion, K_{cu} and K_{bu}=uplift coefficients, D=depth, γ=soil unit weight, B=diameter, W=pile weight, and Ψ=applied load inclination(measured from the upward vertical axis). For rigid rough circular shafts under axial uplift, α=1, $K_{cu}=\pi$, and $K_{bu}=0$ for undrained analyses($\phi=0$). For laterally-loaded shafts in clay, K_{cu} varies from about unity for very short piles to three for long piles.

From an analysis for rigid anchors with constant sections and the results of model tests in both clay and sand, an approximate parabolic interaction relationship was proposed between the inclined uplift capacity ($P_{\psi u}$) and the two limits of axial uplift (Q_u) and lateral capacity (H_u), as given below[17]:

$$P_{\psi u}\cos\Psi/Q_u+(P_{\psi u}\sin\Psi/H_u)^2 = 1 \qquad (4)$$

in which Q_u=axial uplift capacity. Detailed methods for evaluating the axial uplift are given elsewhere[11].

Figure 2 illustrates Equations 2 and 4 in the from of a polar diagram, which gives the foundation capacities for various applied load inclinations. The load eccentricity (e) results in reduction of the lateral component of inclined capacity($P_{\psi u}\sin\Psi$) and, in turn, results in

reduction of the resultant inclined capacity. Details on the eccentricity effects on the inclined capacity are given elsewhere[5].

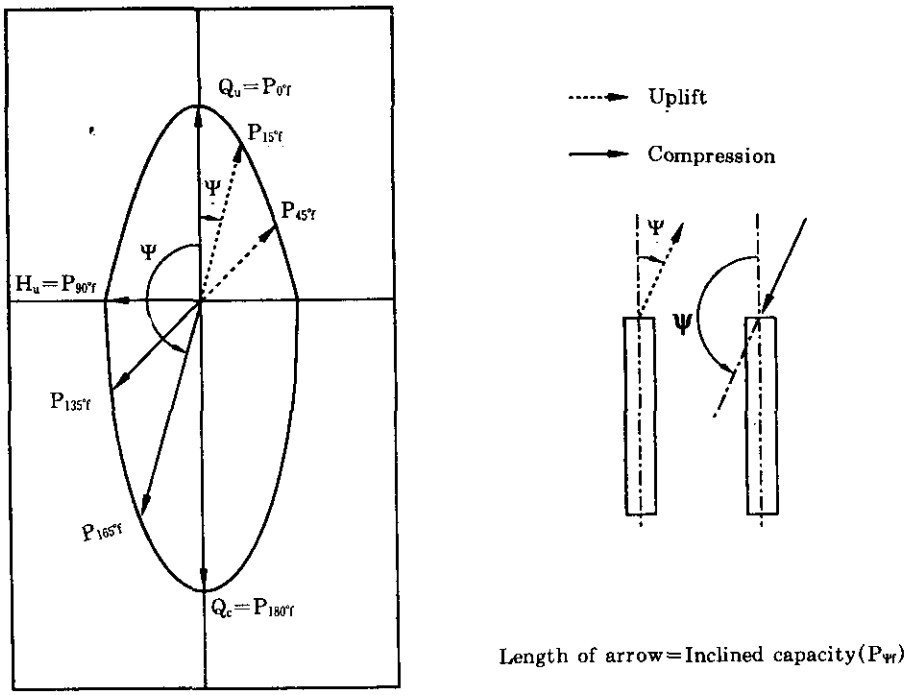

Figure.2 Schematic of polar capacity diagram and load inclination definition

3. Preparation of Laboratory Clay Deposit

Soil deposits were prepared in (a) a short tank, 1.35m diameter by 1.21m high and (b) a tall tank, 1.37m diameter by 2.13m high. The slurry consolidation method was chosen for the preparation of clay deposits because it is the best process satisfying the required degree of uniformity, saturation, and control over stress history[15].

3.1 Material Selection

A mixture containing 50 percent kaolin clay and 50 percent silica was chosen for soil deposit preparation by considering several factors, such as (a) cost of material, (b) consistency, (c) gradation, (d) permeability, (e) consolidation time, (f) surcharge required for consolidation, and (g) compressibility of soil[15]. Grain size distributions for the kaolin, silica, and Cornell clay are shown in Figure 3. For this particle size distribution, Cornell clay is categorized as a clayey silt in which approximately 33 percent of the particle sizes are clay colloids(smaller than 0.002mm), 62 percent are silt size(between 0.074mm and 0.

002mm), and the remaining 5 percent are fine sand(larger than 0.074mm). Table 1 summarizes the index properties of Cornell clay.

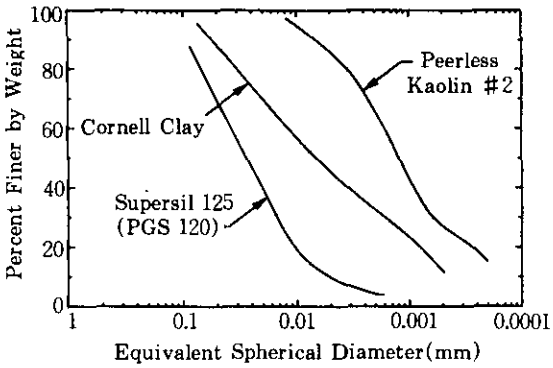

Figure.3 Particle size distribution of cornell clay and slurry constituents

Table 1 Index properties of cornell clay[14]

Property	Symbol	Value
Liquid limit	W_L	33%
Plastic limit	W_p	22%
Plasticity index	PI	11
Specific gravity	G_s	2.65
Percent fines(< #200 sieve)	F	95%
Clay fraction(<0.002mm)	CF	33.3%
Activity(PI/CF)	A	0.33

3.2 Considerations in Soil Deposit Simulation

Natural soils are formed mostly under anisotropic consolidation, in which different effective principal stresses have been applied. This anisotropic consolidation is assumed commonly to be one-dimensional without horizontal strain, and it is denoted usually as consolidation under K_0 conditions. In the laboratory, these K_0 conditions can be simulated by one-dimensional consolidation in fixed-wall chambers in which lateral soil strain is zero. Details on K_0 are given elsewhere[10, 12].

Two major problems associated with soil deposit preparation in the laboratory are:(a) there might exist some difficulties in increasing the overburden stresses and (b) the prepared soil deposit might have a rather high overconsolidation ratio (OCR) profile. The problem associated with the low overburden stresses can be solved partially by prestressing the clay by using high fluid pressure. Some researchers[15, 22] have tried to simulate low OCR profiles without major increases in soil deposit size. However, some difficulties were encountered in maintaining a surcharge stress during either constructing shafts or test loading. One suggestion was to use large chambers and model shafts to minimize the problem of the high OCR profiles[14].

3.3 Adopted Method of Soil Deposit Simulation

For this study, the clay deposits were prepared in three stages:(a) slurry mixing, (b) consolidation, and (c) rebound. Soft and saturated slurry, which was obtained by using a slurry mixing system, was pumped into large fixed-wall chambers. The detailed procedure for mixing slurry is described elsewhere[5, 15]. The slurry was consolidated and brought to a

soft clay deposit consistency. Subsequently, the clay deposit was allowed to rebound by removal of the overburden stress. These three phases currently are the most desirable simulation of clay deposits and could provide advantageous soil characteristics, such as homogeneity, uniformity, saturation, consolidation under K_0 conditions, and proper strengh[14].

4. Consolidation Results

The preconsolidation stres was $48kN/m^2$ for all the of deposits prepared in this study. During consolidation, the soil settlement was measured to monitor the consolidation process. After completion of primary consolidation, the prestress was removed to allow the soil deposit to rebound for several days before the construction of the drilled shafts. Water contents and miniature vane tests were conducted for each drilled shaft during excavation. After the loading tests, each soil deposit was investigated by miniature cone and piezoprobe tests. The data from the water content, vane, cone, and piezoprobe tests were used to characterize and evaluate the quality and physical properties of each soil deposit.

4.1 Consolidation Time

The primary consolidation time was predicted using the consolidation coefficient (c_v) given previously[15], which decreases from 0.2×10^{-6} to $2.0\times10^{-6}m^2/sce$ as the water content increases from 25 to 50 percent. A representative value of c_v during the whole consolidation period was taken to be $0.4\times10^{-6}m^2/sec$, because the initial and final coefficients of consolidation were about 0.1×10^{-6} and $0.7\times10^{-6}m^2/sec$ at the corresponding water contents of about 60 and 37.2 percent, respectively. The coefficients of consolidation also were back-calculated using the log time method(Casagrande's method) and the square root of

Table 2 Consolidation time for soil deposits

Deposit No.	Thickness (mm)	Consolidation Time (mm)		Coefficient of Consolidation, c_v ($10^{-6}m^2/sec$)		
		Predicted[a]	Measured	Assumed[b]	Calculatd	
					C[c]	T[d]
S1	940	9204	6530	0.4	0.67	0.76
S2	990	10416	12022	0.4	0.45	0.68
T1	1940	39204	30903	0.4	0.35	0.38
T2	1880	36817	20184	0.4	0.47	0.58
T3	1860	36038	19055	0.4	0.54	0.62
T4	1900	37604	27542	0.4	0.48	0.53

a-$t=H^2/c_v$ in which H=half of soil deposit thickness and $c_v=0.4\times10^{-6}m^2/sec$

b-assumed representative c_v of whole consolidation period

c-calculated by Casagrande's method

d-calculated by Taylor's method

time method(Taylor's method). Table 2 summarizes te consolidation data.

4.2 Water Content and Vane Shear Tests

The average water content and vane strength from 142 test sets were 37.2 percent (S.D. =1.17 percent) and 8.1 kN/m^2 (S.D.=1.77 kN/m^2), respectively. The coefficient of variation of water contents obtained from this study, which is about 3 percent, indicates relatively consistent and uniform conditions of soil deposits throughout the whole test program[21].

4.3 Cone Penetration Tests and Piezoprobe Tests

Cone penetration tests (CPTS) and piezoprobe soundings were performed using a miniature electric cone penetrometer and piezoprobe built at Cornell. After completion of the load tests, all of the clay deposits were subjected to miniature CPT and piezoprobe soundings. It was necessary to perform the piezoprobe tests together with the CPTS to correct the cone resistance properly. Details of the test procedures and test profiles from each deposit are given elsewhere[5].

For Cornell clay, the average of the measured tip resistance (q_c) and calculated vertical total stress (q) at a depth of 250mm are 58.3 kN/m^2 and 4.5 kN/m^2, respectively. Since the average undrained vane strength(s_{uvm}) is about 8 kN/m^2, the average empirical cone factor [N_c(FV)] at a depth of 250mm is 6.7. This average N_c(FV) value is in the range of N_c(FV) found by others[2]. The average N_c(FV) from this study is close to the lower limit (about 5), because laboratory soil deposits are shallower than most situations in the field.

5. Model Testing Program

5.1 Construction of Model Drilled Shafts

The shafts had an effective diameter (B) of 89mm, while the depths (D) were varied. Since the common range of D/B for transmission line structure foundations is 3 to 10, D/B ratios of 3, 6, and 9 were selected for this study. The shaft construction procedures include : (a) excavating a hole using a hand auger, (b) aligning a single threaded stainless steel reinforcing rod in the open excavated hole, (c) placing a microconcrete mix into the excavated hole, and (d) setting up the direct current differential transformers (DCDTS) and inclinometer. A special microconcrete mix was used because scaled aggregate sizes were necessary to facilitate placement in the small excavation size[13]. A superplasticizer also was added to increase workability during handling and placement. The constituents of the mix consisted of water, Type I cement, fine aggregate, and coarse aggregate in proportions of 6:1.0:2.4:1.7 by weight, respectively. Details on the shaft construction procedures are given elsewhere[5].

5.2 Loading System and Testing Facilities

Load tests were conducted using a servo-controlled hydraulic actuator controlled by a hydraulic pump station, manufactured by Minneapolis Testing Systems(MTS) Corporation. An MTS master controller unit can control the loading modes, range of loading, and rate of loading of the actuator. The actuator unit consisted of a Dayton model 4Z633, which has a total stroke of approximately±50mm and full capacity of 4500N. Loads were measured using a Model JP-1000 load cell, manufactured by Data Instruments, Inc. At the actuator level, a TransTek model J-6 linear variable displacement transducer(LVDT)monitored displacements. The actuator and LVDT were mounted on a steel plate base that was designed to be swung about an upper hinge made between two parallel triangular aluminum plates. The test system was linked to a Hewlett-Packard HP 1000, A900 series mini-computer. Peripherals were interfaced to the computer to facilitate an automated testing procedure. For all of the static tests, the loading rate was fixed at 1.0mm/min, which allowed enough readings to be taken during the entire test.

5.3 Data Acquisition and Reduction

Data acquisition was automated. The data file was stored on the HP 1000 hard disk, and later it was downloaded to a personal computer for manipulation. To infer the horizontal and vertical movement of the shaft butt, the data were reduced further. The actual shaft horizontal and vertical displacements, as well as the apparent depth of rotation (ADOR), were calculated from the shaft geometry and rotation angle measured by the inclinometer.

6. Response of Model Drilled Shafts to Inclined Loads

Twelve inclined static compression and uplift tests were conducted to develop an understanding of the behavior of drilled shafts under static inclined loads. The detailed individual static load test results, including load versus displacement, horizontal load component versus rotation, and normalized apparent depth of rotation versus horizontal displacement, are given elsewhere[5]. The effects of shaft geometry and load inclination on the undrained response of drilled shafts to inclined compression load are pressented briefly in this paper.

The lateral/moment limit method[7], which had been developed originally for interpreting the lateral failure load, was adopted to interpret the failure loads from the inclined load tests. Once the horizontal component load at failure is interpreted, the vertical and resultant applied load at failure could be back-calculated from trigonometry. This method has already been shown to be useful for interpreting inclined load tests in sand[24]. The detailed procedures for interpretation are given elsewhere[5]. Table 3 summarizes the interpreted failure loads and the apparent depths of rotation normalized by depth(ADOR/D) at the corresponding interpreted failure loads for the inclined compression and uplift tests.

Table 3 Summary of static inclined compression and uplift tests

Test Code[a]	Average Vane Strength, s_{uvm}(kN/m²)	Average Water Content, w_{nm}(%)	Applied Load Inclination, Ψ(degrees)	Interpreted Failure Load, $P_{\Psi f}$(N)	ADOR/D at Interpreted Failure Load
S3B135	7.3	37.5	135	340	0.62
S3B165	6.3	37.3	165	541	0.76
S6B135	8.3	371.	135	806	0.62
S6B165	8.2	37.1	165	1121	0.74
S9B135	10.8	36.4	135	1385	0.31
S9B165	7.0	37.5	165	1627	0.44
S3B015	6.5	37.7	15	346	0.77
S3B015	8.6	36.9	45	310	0.53
S6B015	7.1	37.3	15	1257	0.70
S6B045	9.1	36.4	45	706	0.23
S9B015	10.0	36.2	15	1441	0.50
S9B045	11.2	36.2	45	1063	0.37

a−Test code indicates : (a) S=static, (b) D=3B, 6B, 9B, (c) load inclination=135, 165, 15, and 45 degrees measured from upward vertical axis
1N=0.225 lb

6.1 Inclined Compression

6.1.1 Effect of Shaft Geometry

To evaluate the effect of shaft geometry on drilled shaft response to inclined load, the resultant load versus displacement curves for all D/B ratios under comparable initial load inclination are compared in Figure 4. As can be seen, deeper shafts have higher initial stiffness and capacity.

The interpreted failure loads normalized by a reference failure load at D/B=6 for each corresponding load inclination were plotted versus D/B in Figure 5. The plot of the

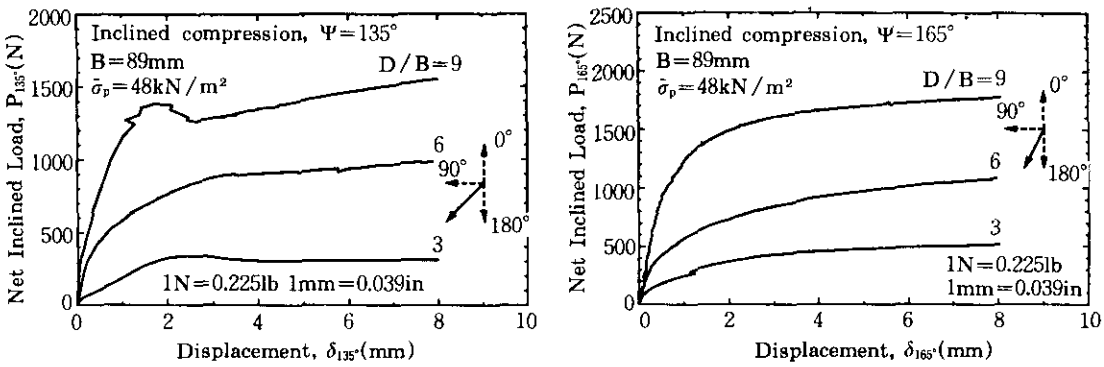

(a) (b)

Figure.4 Effect of shaft geometry on inclined compression response for (a) Ψ=135 and (b) Ψ=165 degrees

normalized undrained inclined compression failure loads at $\Psi=135$ and 165 degrees versus D/B could be compared with the results from the inclined load tests in sand[24]. A linear fit is shown for reference. As can be seen, the normalized failure load in clay increased as D/B increased, just as in sand. Note that the rate of failure load increase with D/B in clay was less than that in sand.

The ADOR/D versus the horizontal displacement components ($\delta_{90°}$) for the same conditions as in Figure 4 are shown in Figure 6. As D/B decreases, the ADOR/D tends to be greater at the same horizontal displacement, up to almost 2mm(0.08 in), probably because of more nonlinearity of load−displacement behavior with shorter shafts. However, the ADOR/D values at larger displacements were more or less the same, except for one test at $\Psi=135$ degrees with D/B=9. The prior study in sand also indicated that shaft geometry does not influence the ADOR/D at larger displacements.

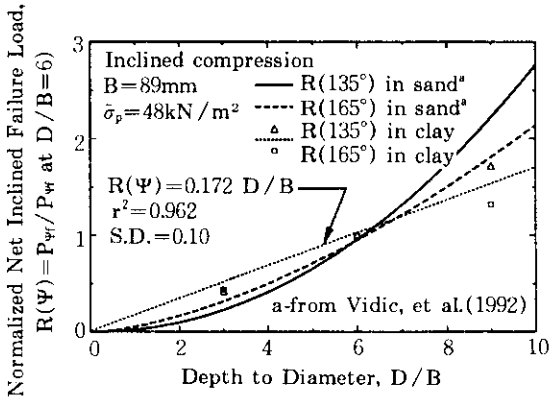

Figure.5 Normalized inclined compression failure load versus D/B

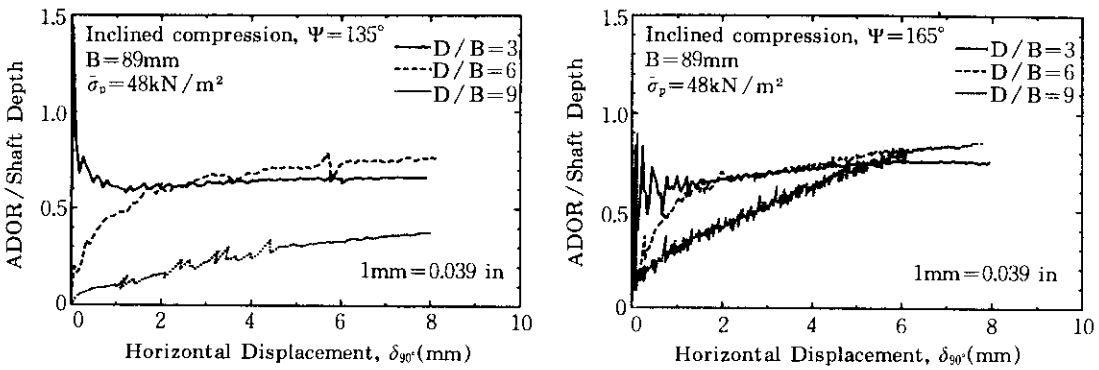

Figure.6 Effect of shaft geometry on ADOR in inclined compression tests for (a) $\Psi=135$ and (b) $\Psi=165$ degrees

6.1.2 Effect of Load Inclination

To evaluate the effect of load inclination, the resultant load−displacement curves for each geometry were plotted, as shown in Figure 7. In addition to the inclined compression test results, the hyperbolic approximation curves for the lateral load tests(Ψ=90 degrees) from previous research[14] were provided for comparison.

As the load inclination (Ψ) increased from 90 to 165 degrees, the initial stiffness and capacity increased. The larger deviation of the applied load from the vertical axis resulted in smaller mobilization of vertical side resistance. Also, a smaller tip resistance might be developed as the load deviation increases from the vertical. The same type of behavior was observed in inclined compression load tests in sand[24].

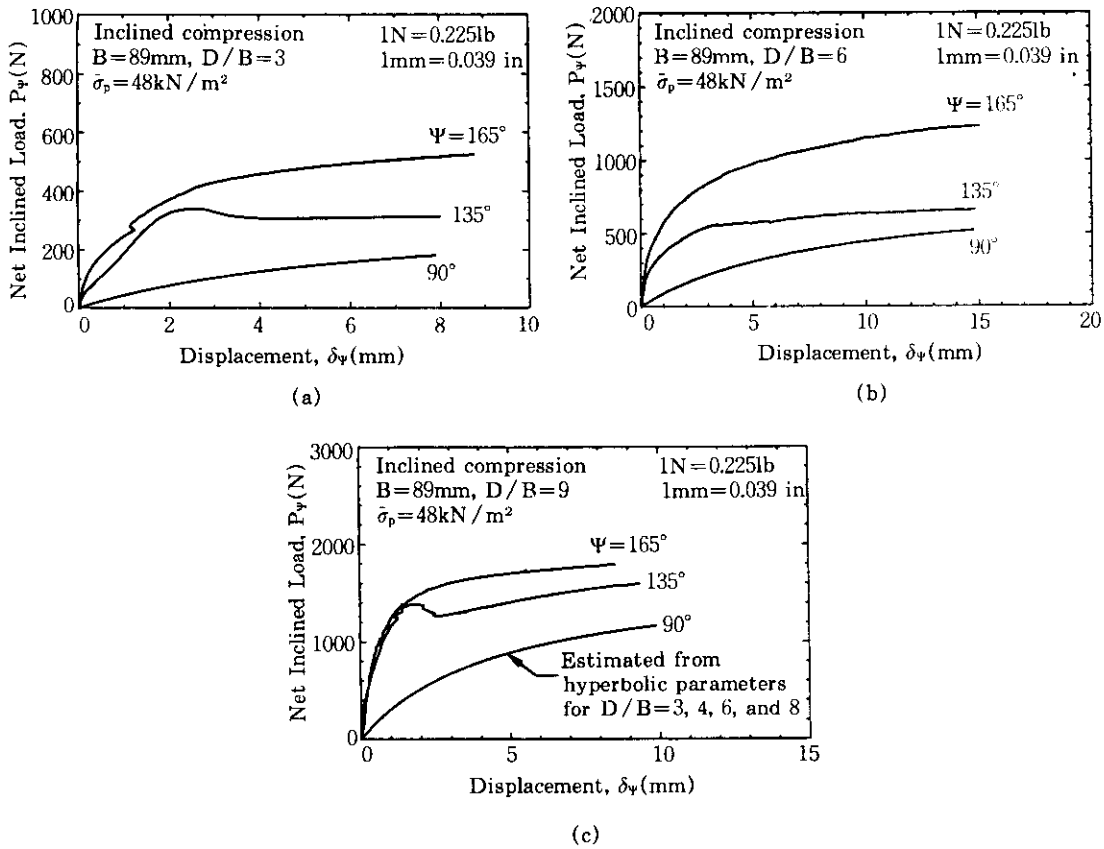

Figure.7 Effect of load inclination on inclined compression response for shafts with (a) D/B=3, (b) D/B=6, and (c) D/B=9

As summarized in Table 3, the ADOR/D for 165 degree compression loading was greater than that for 135 degree loading. This finding also coincides with the previous study[24], in which it was found that the point of rotation moved downward to the tip as the applied load deviated less from the vertical. When a shaft is subjected to inclined compression, in

addition to the moment with respect to the point of rotation produced by the horizontal load component, the nonuniform tip resistance stress and nonsymmetric side resistance produce a moment that has the same sense of rotation as the moment affected by the horizontal load component. The moment added by the vertical component of nonsymmetrical resisting forces could be compensated only by the counteracting moment resulting from the lateral soil restraint by increasing the ADOR. Therefore, the less the load inclination deviates from the vertical. The higher the moment produced by the vertical nonsymmetric resistance will be at the same shaft rotation, which will result in lower point of rotation.

6.2 Inclined Uplift

For inclined uplift tests, care must be taken to separate the effective weight of the shaft plus the hook-up equipment and attached instrumentation from the measured load. Some suction forces likely occur at the interfaces between the upper front or lower back and tip interfaces of the shaft and clay during inclined uplifting loading. However, less suction than during axial uplift loading is expected in inclined uplift tests because the lateral component of inclined load causes the shaft to rotate, resulting in cracks and gaps at the shaft-clay interfaces. Note that the peak suction forces measured at the tip in axial uplift tests were less than 5 percent of net axial uplift capacity.

6.2.1 Effect of Shaft Geometry

The resultant load versus displacement curves for all D/B ratios under comparable initial load inclination are compared in Figure 8. As can be seen, deeper shafts have higher capacity and generally higher initial stiffness like inclined compression tests. As shown in Figure 8b, the load-displacement curve for the shaft with D/B=9 indicates that there might have been some unknown factors present possibly caused by nonuniform shaft construction or soil nonuniformity.

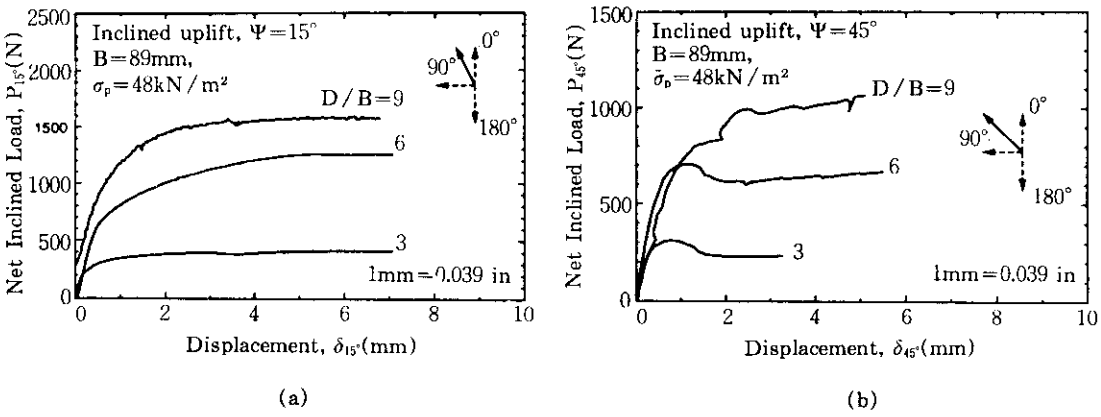

Figure.8 Effect of shaft geometry on inclined uplift response for Ψ=15 and Ψ=45 degrees

The interpreted failure loads normalized by a reference failure load at D/B=6 for each corresponding load inclination were plotted versus D/B in Figure 9. The plot of the normalized inclined uplift failure loads at Ψ=15 and 45 degrees versus D/B can be compared with the results from the inclined load tests in sand[24]. A linear fit is shown for reference. As can be seen, the normalized failure load in clay increased as D/B increased, just as in sand. However, the rate of inclined uplift failure load increase with D/B ratio in clay was less than that in sand, and the same trend also was found in the inclined compression test results.

The apparent depth of rotation normalized by depth(ADOR/D) versus the horizontal displacement component ($\delta_{90°}$) for the same conditions as in Figure 8 are shown in Figure 10. The same trend of geometry effect on ADOR/D was found as in the inclined compression tests

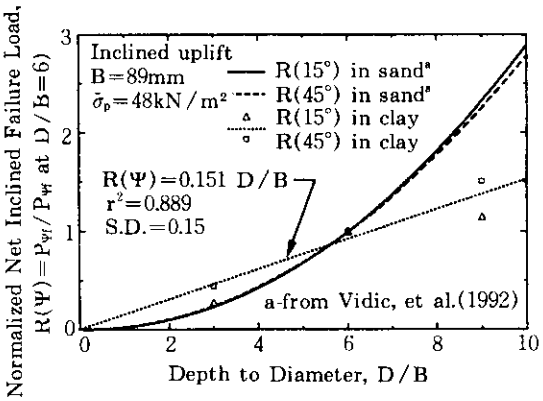

Figure.9 Normalized inclined uplift failure load versus D/B

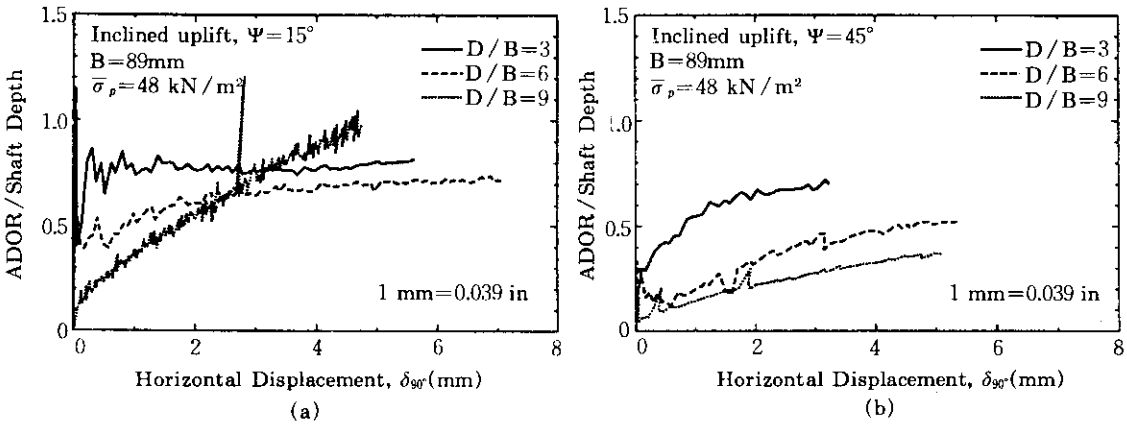

Figure 10. Effect of shaft Geometry on ADOR in inclined uplift tests for (a) Ψ=15 and (b) Ψ=45 degrees

6.2.2 Effect of Load Inclination

The resultant load−displacement curves for each geometry were plotted also to investigate the load inclination effect, as shown in Figure 11. In addition to the inclined uplift

test results, the hyperbolic approximation curves for the lateral load tests(Ψ=90 degrees) from previous research[14] were also provided for comparison.

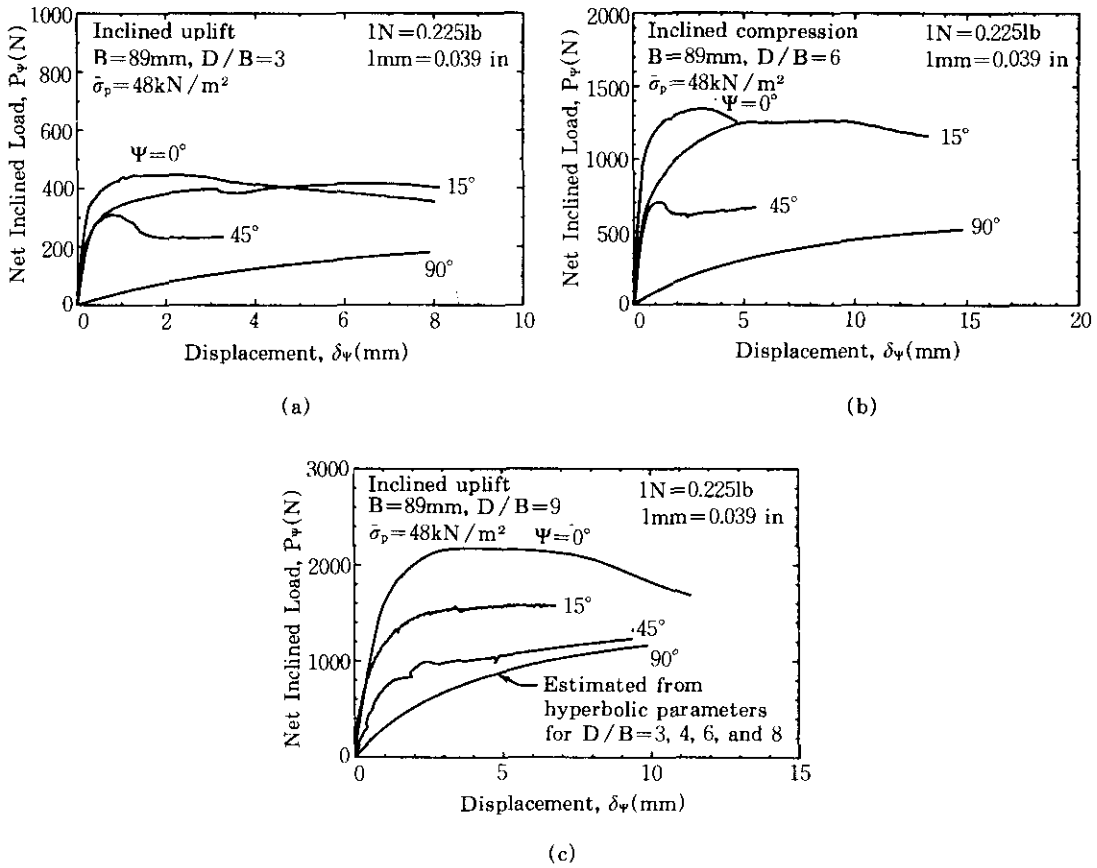

Figure.11 Effect of load inclination on inclined uplift response for shafts with (a) D/B=3, (b) D/B=6, and (c) D/B=9

As the load inclination (Ψ) increased from 0 to 90 degrees, the initial stiffness and capacity decreased. The larger deviation of the applied load from the vertical axis resulted in smaller mobilization of vertical side resistance. The same type of behavior was observed in inclined uplift load tests in sand[24].

As summarized in Table 3, the normalized ADOR for 15 degree uplift loading was greater than that for 45 degree loading. This finding also coincides with the previous sand study [24], in which it was found that the point of rotation moved downward to the tip as the applied load deviated less from the vertical. This finding can be explained in the same manner as described previously.

7. Prediction of Inclined Capacity

The vertical and horizontal components of the resultant inclined failure load must be functions of both the vertical and horizontal failure loads, load inclination, and, probably, the D/B ratios. Unfortunately, there has been no theory to establis these functions considering all of the probable factors. Therefore, only the major factors that could be derived from the load test results were consiered at this time. Simplified functions for calculating each component were established by assuming that the vertical and horizontal components of inclined failure load are functions of the axial and lateral capacity, respectively, and the load inclination as follows:

For inclined uplift:

$$P_{0°@failure} = P_{0°f}\, f_u(\Psi) = Q_{su}\, f_{su}(\Psi) + W_e \tag{5}$$

$$P_{90°@failure} = P_{90°f}\, h_u(\Psi) = H_u\, h_u(\Psi) \tag{6}$$

For inclined compression:

$$P_{180°@failure} = P_{180°f}\, f_c(\Psi) = Q_{sc}\, f_{sc}(\Psi) + Q_{tc}\, t_c(\Psi) \tag{7}$$

$$P_{90°@failure} = P_{90°f}\, h_c(\Psi) = H_u\, h_c(\Psi) \tag{8}$$

in which $P_{0°@failure}$ = vertical component of inclined uplift failure load, $P_{0°f}$ = axial uplift failure load, Q_{su} and Q_{sc} = side resistance under axial uplift and compression, respectively, Ψ = load inclination increasing from 0 degrees in axial uplift to 180 degrees in axial compression, W_e = effective shaft weight, $P_{90°@failure}$ = horizontal component of inclined failure load, $P_{90°f} = H_u$ = lateral failure load, $P_{180°@failure}$ = vertical component of inclined compression failure load, $P_{180°f} = Q_c$ = axial compression failure load, Q_{tc} = tip resistance under axial compression, $f_u(\Psi)$ and $h_u(\Psi)$ = determinant functions of axial and horizontal components in inclined uplift, respectively, $f_c(\Psi)$ and $h_c(\Psi)$ = determinant functions of axial and horizontal components in inclined compression load, respectively, and $f_{su}(\Psi)$ and $f_{sc}(\Psi)$ = determinant functions of side resistance in inclined uplift and inclined compression, respectively.

The determinant functions [$f_{su}(\Psi)$ and $f_{sc}(\Psi)$] for side resistance are assumed to be the same for both inclined uplift and compression cases at the same deviation angles from the vertical [for example, $f_{su}(15°) = f_{sc}(165°)$]. To evaluate the effect of load inclination on tip resistance in inclined compression, a tip resistance determinant function of $t_c(\Psi)$ is also necessary. Tip resistance in inclined uplift is neglected as in axial uplift loading.

To evaluate the determinant functions, the resultant inclined failure load interpreted by the lateral/moment limit method is divided into the vertical and horizontal components and is investigated separately. Figure 12a shows the vertical components of the inclined failure loads, normalized by the comparable axial uplift failure loads, versus the load inclination (Ψ). The relationship between the normalized vertical components of the inclined uplift failure loads and the load inclination can be approximated as follows:

$$P_{0°@failure} / P_{0°f} = (90° - \Psi) / 90° \tag{9}$$

Since the side resistance of rigid drilled shafts under undrained inclined uplift loads is assumed to be the same as that under inclined compression at the same deviation angles from the vertical, the difference between the dotted and solid curves in inclined compression in Figure 12a represents the tip resistance. The tip resistance versus load inclination from a nonlinear regression analysis can be expressed as follows($r^2=0.812$):

$$Q_{tc\Psi} = [(\Psi/90^\circ)-1]^{7.3}Q_{tc} \text{ (for } 90^\circ \le \Psi \le 180^\circ) \tag{10}$$

in which $Q_{tc\Psi}$=tip resistance under inclined compression load and Q_{tc}=tip resistance under axial compression.

A similar approach is used to obtain the determinant functions for the horizontal load components. Figure 12b shows the horizontal components of the inclined failure loads, normalized by the comparable lateral failure loads, versus load inclination. From nonlinear regression analyses, the relationships between the normalized horizontal components of the inclined failure loads and the load inclination can be approximated as follows:

For uplift($0^\circ \le \Psi \le 90^\circ$, $r^2=0.961$):

$$P_{90^\circ@failure}/P_{90^\circ f}=0.953\sqrt{\sin\Psi} \tag{11}$$

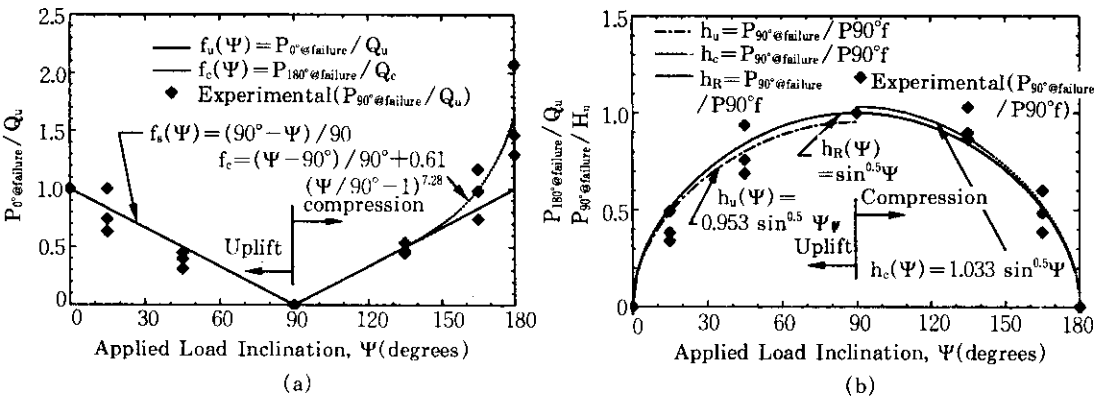

Figure.12 Normalized (a) vertical and (b) Horizontal load components of inclined capacity versus applied load inclination

For compression($90^\circ \le \Psi \le 180^\circ$, $r^2=0.971$):

$$P_{90^\circ@failure}/P_{90^\circ f}=1.033\sqrt{\sin\Psi} \tag{12}$$

For both uplift and compression($0^\circ \le \Psi \le 180^\circ$, $r^2=0.920$):

$$P_{90^\circ@failure}/P_{90^\circ f}=0.995\sqrt{\sin\Psi} \approx \sqrt{\sin\Psi} \tag{13}$$

in which $P_{90°@failure}$=horizontal component of inclined failure load, $P_{90ff}=H_u$=lateral failure load, and Ψ=load inclination. As shown in Equations 11 through 13, the lateral component of undrained inclined uplift is a little bit less than that in compression at the same deviation angles from the vertical.

From Equations 5 through 13, the resulting determinant functions are found as follows:

$$f_{su}(\Psi) = (90°-\Psi)/90° \tag{14}$$

$$f_{sc}(\Psi) = (\Psi-90°)/90° \tag{15}$$

$$h_u(\Psi) \approx h_c(\Psi) \approx \sqrt{\sin\Psi} \tag{16}$$

$$t_c(\Psi) = [(\Psi/90°)-1]^{1.3} \tag{17}$$

The horizontal and vertical components of inclined capacity normalized by the horizontal and vertical capacities, respectively, are shown in Figure 13a. Note that the vertical components of inclined compression and uplift capacities are normalized by the axial compression capacity (Q_c) and the axial uplift capacity (Q_u). Axial-dominated failure will occur when the ratio of the vertical component of inclined capacity to the axial capacity is larger than that of the horizontal component of inclined capacity to the horizontal capacity (Zones A and C). Lateral-dominated failure (Zone B) occurs when the ratio of the horizontal component to the horizontal capacity is larger than that of the vertical component to the vertical capacity. Therefore, if the load inclination measured from the vertical is less than about 30 degrees or greater than about 160 degrees, the axial failure mechanism dominates. For example, an axial-dominated failure mechanism is expected in lattice tower structure foundations because of the geometry of the transmission line structure. When this mechanism is known and understood, the designer must focus on improving the axial capacity of the foundation rather than the latral capacity.

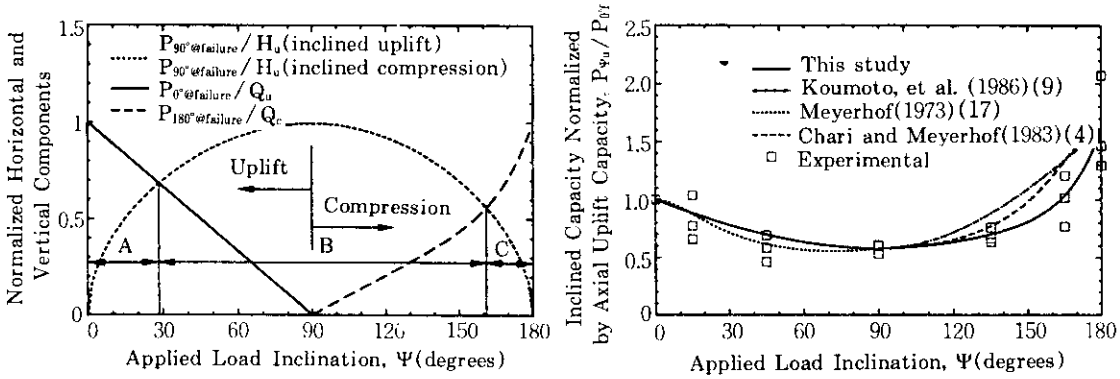

Figure.13 (a) Dominant failure mechanism based on capacity criteria and (b) comparison of inclined capacities predicted by structural interaction formula and new developed equation

The undrained inclined capacity for a given load inclination can be calculated by the simplified determinant functions and the known axial and lateral capacities. Figure 13b shows the inclined capacity versus load inclination calculated by these determinant functions and those suggested by others[4, 9, 17]. The ratios of H_u/Q_u and Q_c/Q_u are 0.60 and 1.6, respectively, in this example. The newly developed equation shows a somewhat less conservative evaluation than the structural interaction formula in inclined uplift loading, while it predicts more conservatively in inclined compression. However, the differences from the different prediction methods are relatively small. A design example using field inclined load test data shows that the new equation yields closer agreement to the test results than others[5].

8. Conclusions

In predicting the inclined capacity of drilled shafts, it is necessary to evaluate first the axial and lateral capacties. They should be interpreted correctly from field data or be calculated by rational methods. Based on the evaluated axial and lateral capacities, the traditional structural interaction formula and/or the newly developed formula can be used. For drilled shafts in clay, the new formula is recommended, because it is developed from specific inclined load test data on drilled shafts. it is not recommended to use the inclination factors, which do not consider the lateral resistance, because the inclined capacity is a combination of the axial and lateral components of the foundation resistance.

It can be very important to predict the dominant failure mechanism of deep foundations under inclined loading. To increase the inclined capacity effectively, the dominant failure component, which is vertical or lateral, should be improved rather than the other.

Acknowledgment

The authors appreciate the assistance of numerous people during the course of this study and want to acknowledge their contributions. H. E. Stewart, K.C. Hover, and C.H. Trautmann of Cornell University provided many useful comments and suggestions. The Electric Powr Research Institute, Palo Alto, California, supported this study under RP 1493.

References

1. Awad, A. and Petrasovits, G., (1968), "Considerations on the Bearing Capacity of Vertical and Batter Piles Subjected to Forces Acting in Different Directions", Proceedings, 3rd Budapest Conference on Soil Mechanics and Foundation Engineering, Budapest, pp. 484~497.
2. Baligh, M.M., Azzouz, A.S., and Martin, R.T.,(1980), "Cone Penetration Tests Offshore the Venezuelan Coast", Report MITSG 80-21, Massachusetts Institute of Technology, Cambridge, 163p.
3. Broms, B.B.,(1965), Discussion of "Piles in Cohesionless Soil Subject to Oblique Pull", Journal of

the Soil Mechanics and Foundations Division, ASCE, 91(SM4), pp. 190~207.
4. Chari, T.R. and Meyerhof, G.G.,(1983), "Ultimate Capacity of Rigid Single Piles under Inclined Loads in Sand", Canadian Geotechnical Journal, 20(4), pp. 849~854.
5. Cho, N.J. and Kulhawy, F.H.,(1995), "Experimental Study of Undrained Behavior of Drilled Shafts During Static and Cyclic Inclined Loading", Report TR-104999, Electric Power Research Institute, Palo Alto, 283p.
6. Hansen, J.B.,(1970), "A Revised Extended Formula for Bearing Capacity", Bulletin No.28, Danish Geotechnical Institute, Copenhagen, pp. 5~11.
7. Hirany, A. and Kullhawy, F.H.,(1988), "Conduct and Interpretation of Load Test on Drilled Shaft Foundations: Detailed Guidelines", Report EL-5915, Electric Power Research Institute, Palo Alto, 374p.
8. Ismael, N.F.,(1989), "Field Tests on Bored Piles Subject to Axial and Oblique Pull", Journal of the Geotechnical Engineering Division, ASCE, 115(GT11), pp.1588~1598.
9. Koumoto, T., Meyerhof, G.G., and Sastry, V.V.R.N.,(1986), "Analysis of Bearing Capacity of Rigid Piles under Eccentric and Inclined Loads", Canadian Geotechnical Journal, 23(2), pp.127~131.
10. Kulhawy, F.H. and Mayne, P.W.,(1990), "Manual on Estimating Soil Properties for Foundation Design", Report EL-6800, Electric Power Research Institute, Palo Alto, 306p.
11. Kulhawy, F.H., Trautmann, C.H., Beech, J.F., O'Rourke, T.D., McGuire, W., Wood, W., and Capano, C.,(1983), "Transmission Line Structure Foundations for Uplift Compression Loading", Report EL-2870), Electric Power Research Institute, Palo Alto, 412p.
12. Mayne, P.W. and Kulhawy, F.H.,(1982), "K_o-OCR Relationships in Soil", Journal of the Goetechnical Engineering Division, ASCE, 108(GT6), pp. 851~872.
13. Mayne, P.W. Hover, K.C., and Kulhawy, F.H.,(1994), "Microconcrete for Model Drilled Shaft Foundations", Construction and Building Materials, 8(2), pp.127~135.
14. Mayne, P.W., Kulhawy, F.H., and Trautmann, C.H.,(1992), "Experimental Study of Undrained Lateral and Moment Behavior of Drilled Shafts During Static and Cyclic Loading", Report TR-100221, Electric Power Research Institute, Palo Alto, 383p.
15. McManus, K.J. and Kulhawy, F.H.,(1991), "Cyclic Axial Loading of Drilled Shaft Foundations in Cohesive Soil for Transmission Line Structures", Report El-7161, Electric Power Research Institute, Palo Alto, 290p.
16. Meyerhof, G.G.,(1963), "Some Recent Research on the Bearing Capacity of Foundations", Canadian Geotechnical Journal, 1(1), pp.16~26.
17. Meyerhof, G.G.,(1973), "Uplift Capacity of Foundations under Oblique Loads", Canadian Geotechnical Journal, 10(1), pp.64~70.
18. Meyerhof, G.G.,(1981), "The Bearing Capacity of Rigid Piles and Pile Groups under Inclined Loads in Clay", Canadian Geotechnical Journal, 18(2), pp.297~300.19. Meyerhof, G.G. and Ranjan, G.,(1972), "Bearing Capacity of Rigid Piles Under Inclined Loads in Sand, I:Vertical Piles", Canadian Geotechnical Journal, 9(4), pp.430~446.
20. Meyerhof, G.G. and Yalcin, A.S.,(1983), "The Bearing Capacity of Rigid Piles and Pile Groups under Eccentricity and Inclined Loads in Clay", Proceedings, 36th Canadian Geotechnical Conference, Vancouver, Canada, pp. 3.1.1~6.
21. Spry, M.J., Kulhawy, F.H., and Grigoriu, M.D.,(1988), "A Probability-Based Geotechnical Site Characterization Strategy for Transmission Line Structures", Report EL-5507, Vol. 1, Electric Power Research Institute, Palo Alto, 103p.
22. Sulaiman, J.I.,(1985), "A Laboratory Study of the Factors Influencing the Development of Shaft Adhesion on Bored Piles in Clays", Ph.D.Thesis, University of Sheffield, UK, 180p.
23. Vesic, A.S.,(1975), "Bearing Capacity of Shallow Foundations", Foundation Engineering Handbook,

Ed, by H. Winterkorn and H.Y. Fang, Van Nostrand Reinhold, New York, pp. 121~147.

24. Vidic, S., Kulhawy, F.H. and Trautmann, C.H.,(1992), "Experimental Study of Drained Behavior of Drilled Shafts During Static Inclined Loading", Report TR-101131, Electric Power Research Institute, Palo Alto, 232p.
25. Vidic, S., Kulhawy, F.H., and Trautmann, C.H.,(1993), "Experimental Study of Drained Behavior of Drilled Shafts During Cyclic Inclined Loading", Report TR-103597, Electric Power Research Institute, Palo Alto, 218p.
26. Yoshimi, Y.,(1964), "Piles in Cohesionless Soil Subject to Oblique Pull", Journal of the Soil Mechanics and Foundations Division, ASCE, 90(SM6), pp.11~24.

(접수일자 1995. 5. 17)